17th World Conference on Earthquake Engineering, 17WCEE
Sendai, Japan - September 13th to 18th 2020

SEISMIC PERFORMANCE OF A FRICTION PENDULUM-GAP DAMPER COUPLED SYSTEM

V. Quaglini [(1)], D. De Domenico [(2)], E. Gandelli [(3)], G. Ricciardi [(4)]

[(1)] *Politecnico di Milano, Italy, virginio.quaglini@polimi.it*
[(2)] *University of Messina, Italy, dario.dedomenico@unime.it*
[(3)] *Politecnico di Milano, Italy, emanuele.gandelli@polimi.it*
[(4)] *University of Messina, Italy, gricciardi@unime.it*

Abstract

Sliding devices with curved surface, also known as Friction Pendulum (FP) bearings, are widely used seismic isolation devices that exploit the self-centering mechanism related to the pendulum operating principle and provide energy dissipation in relationship to the frictional characteristics of the sliding interface. Displacement demand, energy dissipation and re-centering capability of FP bearings are affected by the frictional properties of the sliding pad. Indeed, higher friction coefficients increase the energy dissipation capability, thus reducing the displacement demand, but worsen the re-centering behavior. Potential residual displacements at the end of the earthquake influence the serviceability of the structure and may also cause accumulation of displacements in aftershocks and future events. On the other hand, FP bearings with lower friction coefficients exhibit a better re-centering behavior, but the corresponding energy dissipation is reduced in comparison with higher-friction FP bearings, which in turn implies higher displacement demand. In an attempt to efficiently combine the good re-centering behavior of low-friction FP bearings with a satisfactory energy dissipation typical of high-friction FP bearings, this contribution presents a friction pendulum-gap damper coupled system. Unlike a conventional damper, the gap damper introduces additional energy dissipation not throughout the range of displacements, but only when a threshold displacement or initial gap is exceeded, while not being engaged otherwise. The gap damper mechanical properties are chosen according to a performance-oriented design procedure, assuming a target displacement demand of the combined isolation system. The design procedure is numerically validated through a parametric study including a series of nonlinear response history analyses, different FP bearing properties, and two intensities of the earthquake excitation (extreme and serviceability) associated with two distinct performance requirements. The results of the parametric study demonstrate that the gap damper is effective in reducing the displacement demand during extreme earthquakes, while not impairing the re-centering capability of the FP bearing, even during minor serviceability earthquakes. Consequently, the proposed system outperforms both the high-friction FP bearings, which suffer from a low re-centering capability, and the low-friction FP bearings, which suffer from large displacement demand.

Keywords: Friction pendulum; Gap damper; Base isolation; Re-centering capability; Friction coefficient.

1. Introduction

Base isolation is a mature technology that has been widely used in earthquake-prone regions to mitigate the seismic response of buildings, bridges and industrial facilities. Traditional isolation devices include elastomeric bearings and sliding (friction-based) devices. The friction-based isolation devices are usually realized with a curved sliding surface that provides the necessary re-centering force due to a simple pendulum mechanism – the so-called friction pendulum (FPS) system [1], also called curved surface slider (CSS). In its basic configuration, the friction pendulum (FP) bearing (or CSS) comprises a concave sliding plate and an articulated slider. The sliding interface is lined by a thermoplastic material, so that energy dissipation via friction is generated during the sliding motion of the slider over the concave plate. The friction coefficient of the sliding material and the effective curvature radius of the concave plate govern the dynamic behavior of the FP bearing. The lengthening of the first-mode period provided by the FPS drastically reduces the earthquake-induced forces and absolute accelerations in the superstructure, but also implies large displacement demand concentrated at the isolation level. Hence, large in-plan dimensions of the FP bearings are necessary to accommodate this displacement demand, which may be huge depending on the seismic hazard of the installation site. A way to reduce the in-plan dimensions of the isolators is to use the Double Friction Pendulum [2] device, having a displacement capacity two times higher than the single FP device because of the engagement of two (generally identical) sliding surfaces contemporaneously. However, the large displacement demand is important also from other design perspectives such as the nonstructural lifelines and utilities, which must be flexible enough to tolerate the isolators' motion without damage, and the risk of collision between adjacent buildings due to the large isolators' displacements [3]. Consequently, an important research topic is concerned with the development of feasible and effective solutions to reduce the displacement demand of the isolation system.

Among the strategies to reduce the displacement demand of the isolators, one obvious solution would be to increase stiffness properties at large displacement. In FP bearing, this may be achieved via a variable friction coefficient and/or a variable radius of curvature along the sliding surface [4], [5]. Other attractive solutions consist in placing a Tuned Mass Damper (TMD) or an inerter-based vibration absorber immediately above or below the isolation layer, so as to realize an effective and robust hybrid isolation system [6]-[9] with improved seismic performance and lower displacement demand for the isolators compared to traditional isolation systems. Alternatively, adaptive energy dissipation alongside alterable deflection constraints are provided by sliding magnetic bearings, which represent promising isolation devices in this context [10], [11].

Besides the displacement demand, another important property of the isolation system is represented by the re-centering behavior, i.e. its capability to return to the original position once the earthquake excitation is concluded. This property is typically quantified by the residual displacement d_{res}. In FP bearings, displacement demand and re-centering capability are two competing properties determined by the friction coefficient at the sliding interface [12]. Indeed, high friction coefficients are associated with low displacement demand due to the higher energy dissipation capabilities, but also result in larger residual displacements (i.e. poor re-centering behavior). In contrast, low friction coefficients produce a good re-centering performance but at the same time imply large displacement demand due to the lower energy dissipation [13], [14]. Based on these fundamental principles, an optimal friction-based isolation system should be based on low-friction sliding materials, so as to guarantee a good re-centering behavior as a whole, but should also include some additional supplemental damping mechanism that prevents the displacements from getting very large during extreme earthquakes. In other words, the supplementary dissipation mechanisms should ideally work for extreme earthquakes only, but not for low-intensity earthquakes. Such desired "displacement-dependent" dissipation mechanism is developed in this study by a gap damper system. The gap damper [15] provides supplemental energy dissipation only for isolators' displacements exceeding a given threshold, called gap displacement d_{gap}, whereas it is not engaged for smaller displacements, typical of serviceability earthquakes. The present paper proposes an effective friction pendulum-gap damper coupled system in order to accomplish different performance requirements depending on the intensity level of the seismic input. A performance-oriented design procedure based on a desired (target) displacement demand of

the combined isolation system under the design earthquake is developed. This procedure is then validated through a series of nonlinear time history analyses for different FP bearing properties, two intensities of the earthquake excitation (extreme and serviceability) associated with two distinct performance requirements. The outcomes of the numerical study results demonstrate that the proposed friction pendulum-gap damper coupled system is effective in reducing the displacement demand during extreme earthquakes, while ensuring a good re-centering behavior of the isolation system, even during minor serviceability earthquakes. As a result, the proposed system shows advantages over both high-friction FP bearings, which suffer from a poor re-centering capability, and low-friction FP bearings, which entail large displacement demand.

2. Gap damper system

The main function of the gap damper is to provide supplemental energy dissipation once the displacement gets higher than a pre-defined threshold, called "gap displacement" d_{gap}. This implies that the gap damper is not engaged for displacements $d < d_{gap}$, meaning that it provides zero reaction force until the gap displacement is exceeded. The development of a dissipation mechanism (related to the arisen reaction force of the gap damper) that is strictly dependent on the displacement amplitude is called "phased behavior" in the literature [15]. In this context, a scheme exploiting the phased behavior of the gap damper coupled with a base isolation system was earlier proposed by Zargar et al. [15]. The latter scheme, whose idealized sketch is reported in Fig. 1, was also investigated through shake table tests by the same authors [16], [17]. The two gap dampers are connected to the CSS isolation system through a rigid steel frame. The internal walls of such frame are separated from the central isolation system by a distance d_{gap} at either side, so that the two gap dampers are not engaged for isolators' displacements lower than d_{gap} (in either side of a unidirectional motion). Although not considered in this paper for brevity, extension to multi-directional motion is straightforward. It was found that this scheme is effective to achieve different performance requirements for different intensity levels of the earthquake excitation, as the gap damper system is able to mitigate the displacements during extreme earthquake events, while not being engaged for low-intensity earthquakes.

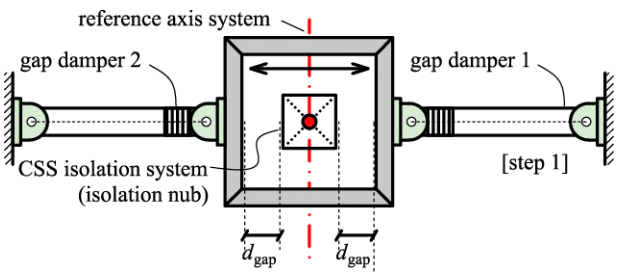

Fig. 1 – Combined base isolation and gap damper system (adapted from Zargar et al. [15])

However, the engagement of the gap damper in Fig. 1 implies a plastic deformation accumulation towards the direction of motion, which may be detrimental for the re-centering behavior of the overall system. For instance, let us assume that a positive plastic deformation is caused by the engagement of gap damper 1 due to a displacement $d > d_{gap}$. This plastic deformation may or may not be recovered at the end of the seismic event. This depends on the nature of the earthquake excitation and on the possible compensation by a negative plastic deformation accumulated by gap damper 2 in the opposite direction, i.e. due to a negative displacement $|d| > d_{gap}$. As an extreme case, a strong asymmetric accelerogram typical of a pulse-like earthquake event with pronounced directivity effects may cause the accumulation of plastic deformation towards a direction, e.g. the right direction. This means that, at the end of the earthquake excitation, the rigid frame would be shifted to the right (i.e., a positive shift to the right is accumulated compared to the original, central position shown in Fig. 1). Obviously, the restoring force of the CSS isolators (related to the curvature radius of the FP bearing) would try to re-center the isolation system, but would be contrasted by the reaction force of the gap damper system in its shifted position. Evidently, the re-centering behavior is negatively

affected by the plastic deformation of the gap damper system, and some permanent displacements may result.

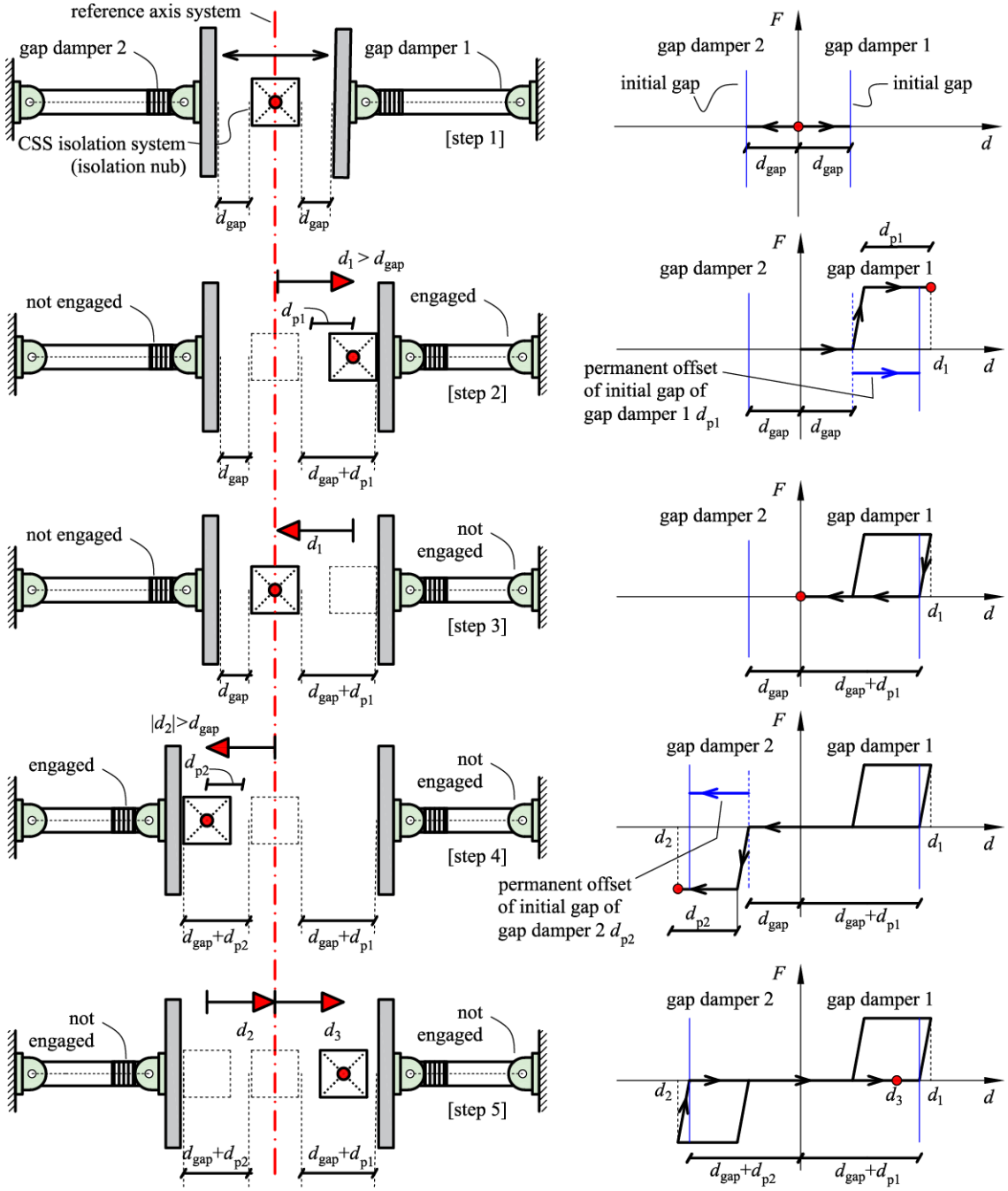

Fig. 2 – Combined base isolation and gap damper system (proposed system) (adapted from [18])

To overcome this drawback, an alternative scheme that does not negatively affect the re-centering behavior of the isolation system is proposed in this paper, as sketched in Fig. 2. A full description of this scheme and its working mechanism can be found in a recent paper by the authors [18]. Similar to the previous gap damper system, the isolation nub is connected to the gap damper system (composed of two hysteretic gap dampers) through some steel (rigid) walls. However, unlike the previous scheme proposed by

Zargar et al. [15]-[17], the scheme in Fig. 2 does not entail a closed rigid steel frame, but two independent steel walls. This different realization feature allows the engagement of one gap damper at a time, depending on the current direction of motion of the CSS isolators. Hence, both the gap dampers in this scheme work as "compression-only" elements. By inspection of the kinematical analysis and the corresponding force-displacement response in Fig. 2, it is clear that the proposed scheme does not generate any reaction force in the neighborhood of the origin, which guarantees the overall re-centering behavior of the isolation system. This is an evident advantage of this scheme in comparison to the previous gap damper scheme in Fig. 1. Nevertheless, it is worth noting that in this case the permanent deformation accumulated by the gap dampers causes a so-called "cumulative damage" of the gap damper system, meaning that the gap displacement does not keep constant during the entire time history, but becomes wider at each gap damper engagement. This effect can be clearly seen by comparing the force-displacement response in step 3 and in step 5. Since the gap damper 1 is previously engaged in step 3, the gap displacement changes (increases) from d_{gap} to d_{gap} + d_{p1}, where d_{p1} represents the plastic deformation accumulated by gap damper 1 in step 3. Therefore, a permanent offset of gap damper 1 of a quantity d_{p1} widens the gap interval for subsequent engagements, so that the engagement of the gap damper may be delayed in aftershocks (as occurs in step 5 in the presented example in Fig. 2). The implications of the cumulative damage on the time history response will be analyzed in the time history analysis discussed in the remainder of the paper.

3. Performance-oriented energy-based design procedure

The hysteretic gap damper is described in this paper by an elastic-perfectly plastic constitutive behavior, characterized by initial stiffness K_i and yield force F_y. The yield displacement is assumed as d_y = 1 mm, thus it is not an explicit design variable. The gap damper is designed through two free variables: 1) the yield force F_y (which directly affects the energy dissipation capability); 2) the gap displacement d_{gap} (which directly affects the engagement point of the additional damping provided by the gap damper). In line with other design procedures applied to other passive control devices, such as viscous dampers [19], the design procedure of the gap damper system is based on energy dissipation concepts. In particular, the procedure aims to identify the value of the yield force F_y of the gap damper system such that the displacement demand of the isolation system decreases from d_{cd} to a desired (target) reduced displacement d_{red}. The reduced displacement is here expressed as a fraction of the initial displacement through the introduction of a reduction factor RF as follows

$$d_{red} = RF \cdot d_{cd} \tag{1}$$

where $0 < RF < 1$. Based on energy balance considerations and with the aid of the idealized sketch in Fig. 3, the energy dissipation of the gap damper (dashed area E_{damper} in Fig. 3) is set equal to the energy dissipation of the low-friction CSS when moving from d_{red} to d_{cd} (dashed area E_{red} in Fig. 3). Hence, the following value of yield force of the gap damper system is obtained

$$F_y = \frac{2F_0\left(1-RF\right)d_{cd}}{RF \cdot d_{cd} - d_{gap} - d_y} \tag{2}$$

where F_0 is the characteristic strength of the CSS isolator, obtained as the product of the friction coefficient μ and the vertical load acting on the bearing N. Eq. (2) represents a closed-form formula for the yield force of the gap damper system according to the proposed performance-oriented energy-based design procedure.

Besides the yield force F_y given in (2), another key parameter for the design of the gap damper system is the gap displacement, which indicates the displacement threshold for the engagement of the gap damper. In previous papers [15]-[17], the gap displacement was chosen such that the supplemental damping is offered only during extreme earthquakes, whereas it is absent during design earthquakes. In contrast, this study

explores different possibilities of the gap displacement d_{gap} and its relevant effect on the seismic performance of the combined system are analyzed, as illustrated in the next section.

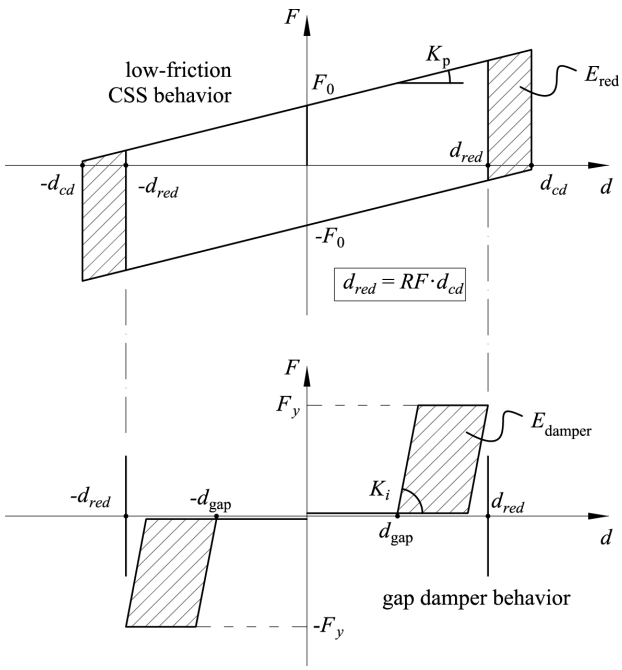

Fig. 3 –Constitutive behavior of low-friction CSS (top) and gap damper (bottom) (adapted from [18])

4. Numerical analyses and seismic performance of the proposed system

Nonlinear response history analyses (NRHAs) are performed to evaluate the seismic performance of the proposed isolation system combining low-friction CSSs and hysteretic gap dampers. Assuming a rigid-body behavior of the superstructure, the model of the isolated structure is represented by a single-degree-of-freedom (SDOF) system. The software framework OpenSees v. 2.5.4 [20] is used for the NRHAs. In particular, the "Single Friction Pendulum Bearing Element" is used for the FP bearings, with a velocity-dependent friction model governed by the following well-known exponential law [21]

$$\mu_d = \mu_{HV} - (\mu_{HV} - \mu_{LV}) \cdot \exp(-\alpha v) \tag{3}$$

where μ_{LV} and μ_{HV} represent low-velocity and the high-velocity friction coefficient, respectively, α is a rate parameter having the dimensions of the inverse of a velocity (assumed as 0.0055 s/mm in this study), and v represents the horizontal velocity. The "elastic-perfectly plastic gap material" (compression only) is used to describe the hysteretic behavior of the gap damper. A constant vertical load equal to $N = 1000$ kN is assumed for all the numerical analyses. An elastic-perfectly plastic bilinear model is assumed for the FP isolators, with initial stiffness 100 times higher than the post-elastic stiffness, so as to minimize the elastic deformation of the CSS. Different radii of curvature and friction coefficient were considered in a broad parametric study, whose full details can be found in [18]. In this paper, only a limited part of the parametric study results is shown and commented. A suite of seven ground motion records for two distinct limit states are selected to be spectrum-compatible with the response spectrum of the site of Lamezia Terme, Italy (latitude 38.57°, longitude 16.18°) provided by the Italian building code NTC2018 [22]. A reference life of the structure equal to 200 years is assumed. Both serviceability limit state (SLD, damage-limitation requirements) and ultimate limit state (SLC, no-collapse requirements) are considered in this study. Finally, three gap factor ratios d_{gap} /

d_{red} equal to 25%, 50% and 75% are chosen (denoted as GF_1, GF_2 and GF_3 in the parametric study, respectively).

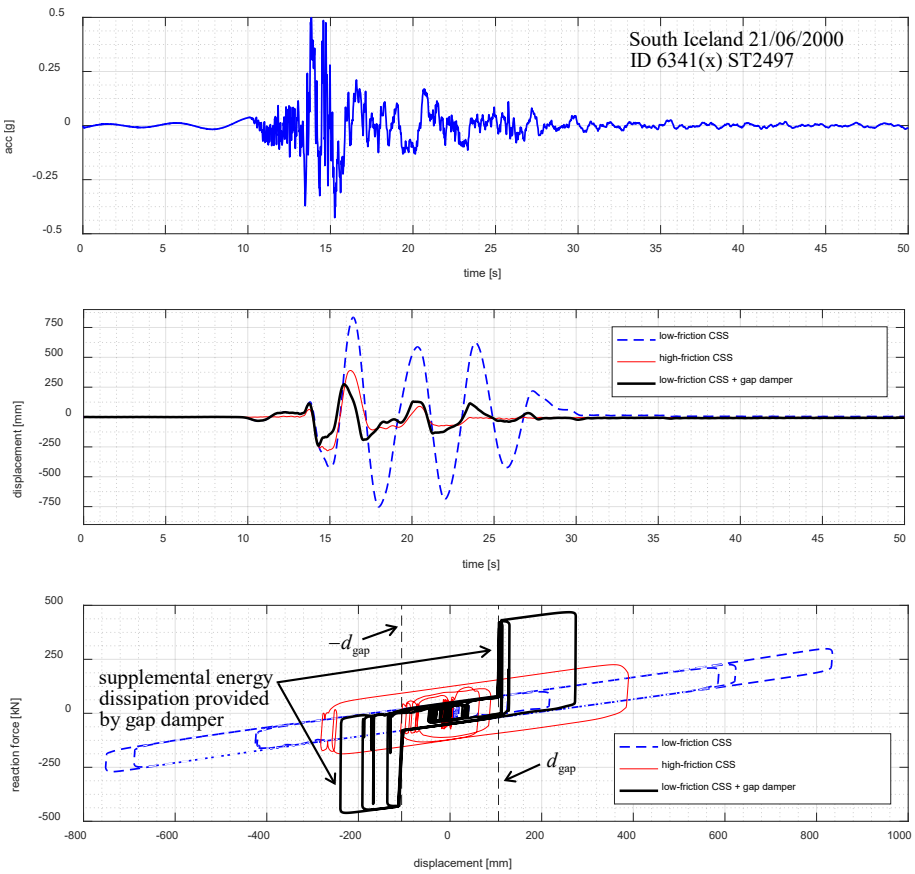

Fig. 4 – High-intensity ground motion acceleration (top), displacement response for three different isolation layouts, including the proposed system (middle) and force-displacement cycles (bottom) (adapted from [18])

An example of time history response under a high-intensity ground motion record (South Iceland earthquake, 21/06/2000) is shown in Fig. 4, considering an FP bearing with effective curvature radius of 3500 mm. The low-friction CSS corresponds to $\mu_{LV} = 0.02$, while the high-friction CSS corresponds to $\mu_{LV} = 0.05$. A ratio $\mu_{HV} / \mu_{LV} = 2.5$ is assumed for all the numerical examples in this study. The gap damper system is designed according to the performance-oriented design procedure illustrated in Section 3, assuming the displacement demand of the high-friction CSS (average response from the 7 records at SLC) as the target displacement d_{red}. Based on the results shown in Fig. 4, it is clearly noticed that the proposed gap damper system is effective in reducing the displacement demand of low-friction CSS to a comparable level to that of the high-friction CSS. The supplemental energy dissipation is engaged only for displacements d exceeding the gap displacement d_{gap} in either direction, as illustrated in the bottom part of Fig. 4.

It is worth noting that the idealized behavior shown in Fig. 4 ignores the cumulative damage of the gap damper, as the force-displacement cycles are the same at first and subsequent engagements, regardless of the previous accumulation of plastic deformation. However, the effect of the cumulative damage in the gap damper system may be detrimental for the seismic performance and cannot be ignored. This effect can be simulated in OpenSees through the option “damage” switched on in the elastic-perfectly plastic gap material [20]. In order to show the impact of the cumulative damage on the seismic performance of the isolation system, Fig. 5 shows a comparison between the displacement response and the corresponding force-displacement cycles. It is clearly seen that the delayed engagement of the gap damper system due to the previous plastic deformation accumulation worsen the displacement mitigation performance, as expected.

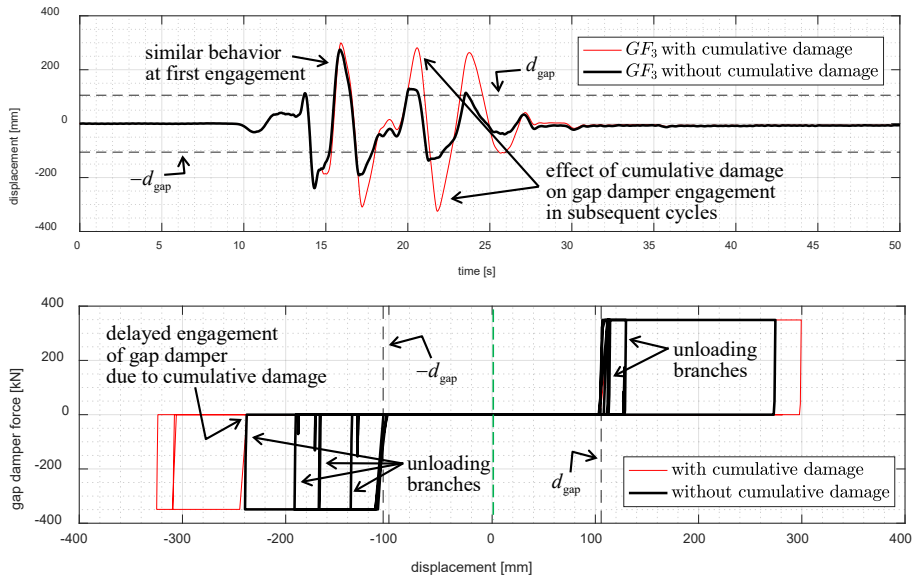

Fig. 5 – Differences in the displacement time history of low-friction + gap damper system with and without cumulative damage (top) and force-displacement cycles (bottom) (adapted from [18])

This is clearly noticed by comparing the displacements before and after the first engagement of the gap damper, namely once the plastic deformation has already started to accumulate. The gap displacement is indeed larger than in the previous cycles, which implies that the gap damper is not engaged until a new (larger) displacement threshold is exceeded. Hence, the supplemental energy dissipation is not provided unless a larger displacement value is achieved. Despite the negative effect of the cumulative damage, the displacement demand of the proposed low-friction + gap damper system keeps much smaller than the displacement demand of the low-friction CSS isolation system alone (cf. again results shown in Fig. 4).

The effect of the gap displacement (or the gap factor *GF*) is analyzed in Fig. 6, where three gap displacements equal to 25%, 50% and 75% of the target displacement d_{red} are compared. Evidently, the most effective choice is represented by the gap factor GF_3 (initial gap equal to 75% of the target displacement). In other words, the most effective choice is to select a larger gap displacement. This results is reasonable for the system with cumulative damage, as this choice would minimize the plastic deformation due to a lower number of engagements of the gap damper system. A larger gap displacement would imply that the gap damper is engaged only for the strong motion phase of the earthquake excitation, where it is expected to be mostly effective. On the contrary, for smaller gap displacements, the gap damper system would be engaged even during small movements of the isolation system, with a resulting accumulation of plastic deformation over the entire response history. Note that the same value of energy dissipation is assumed for the three gap factors (according to the energy-based design procedure explained in Section 3). Therefore, lower gap displacements entail lower values of yield force and higher displacements. A clear difference in the force-displacement curves can be noticed by comparing the cases with and without cumulative damage. Indeed, the increase of the gap factor in subsequent cycles (following the first engagement) due to the cumulative damage results in larger displacements to dissipate the same amount of energy.

Finally, the seismic performance of the proposed low-friction CSS + gap damper system is analyzed under a low-intensity ground motion, typical of serviceability earthquakes (Golbasi earthquake, 05/05/1986). The displacement time history is purposely reported for a longer time duration than the duration of the considered ground motion record, so as to investigate the residual displacement at the end of the earthquake. As can be seen, the residual displacement for high-friction CSS isolation system under a low-intensity ground motion may be high, in the present case 21 mm that is around 60% of the peak displacement (32 mm). On the contrary, the proposed low-friction + gap damper system is characterized by a good re-centering behavior, and the residual displacement is basically the same as the low-friction CSS isolation system alone. Similar considerations can be made in terms of the absolute acceleration response. Indeed, the

peak accelerations of the proposed low-friction CSS + gap damper system are of comparable order as those of the low-friction CSS isolation system alone, and much lower (around halved) than those of the high-friction CSS isolation system alone. This emblematic example, relevant to an arbitrary serviceability earthquake, demonstrates the advantages of the phased behavior provided by the gap damper in eliminating undesirable effects of high-friction FP bearings for low-to-moderate intensity earthquake excitations. Similar results are obtained for the other ground motion records of the parametric study [18], here not shown for brevity.

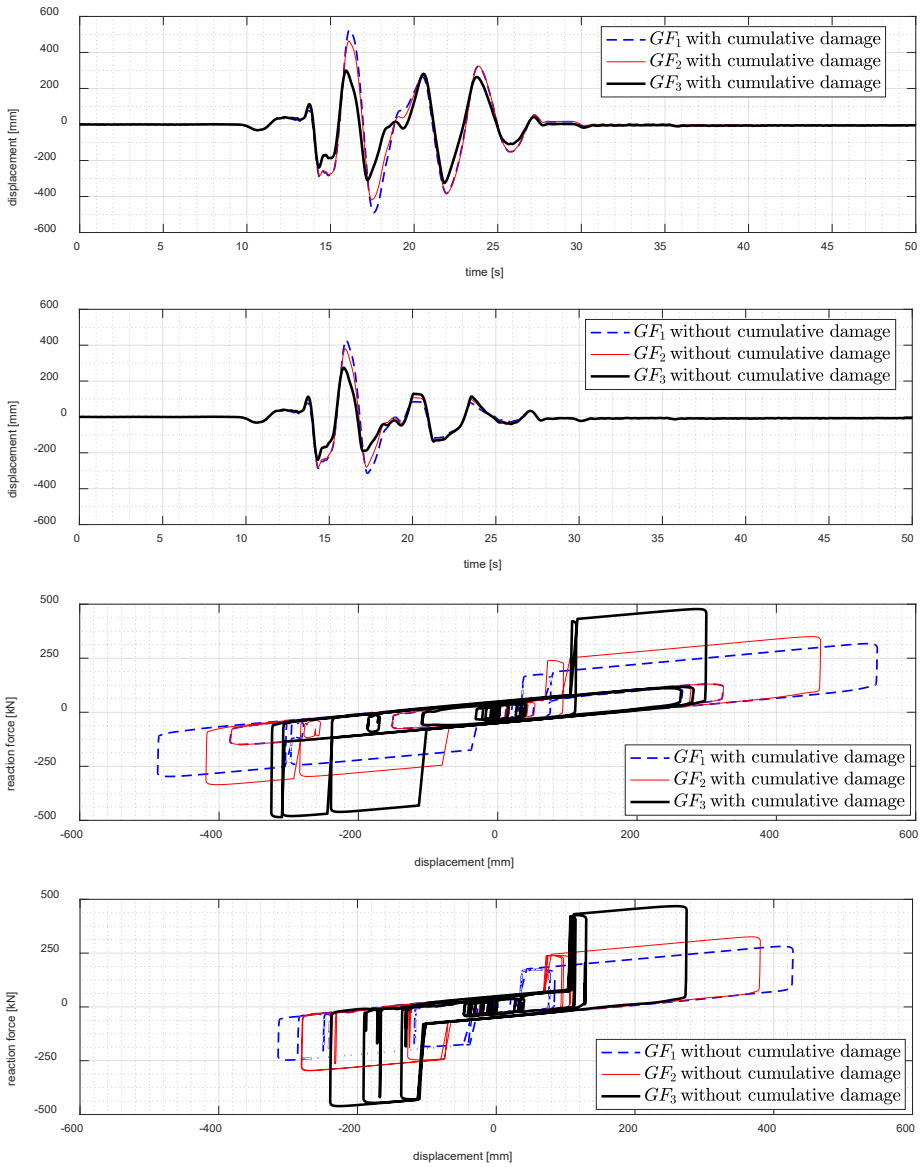

Fig. 6 – Displacement time history (top) and force-displacement cycles (bottom) of low-friction + gap damper system depending on gap factor *GF*, with and without cumulative damage (adapted from [18])

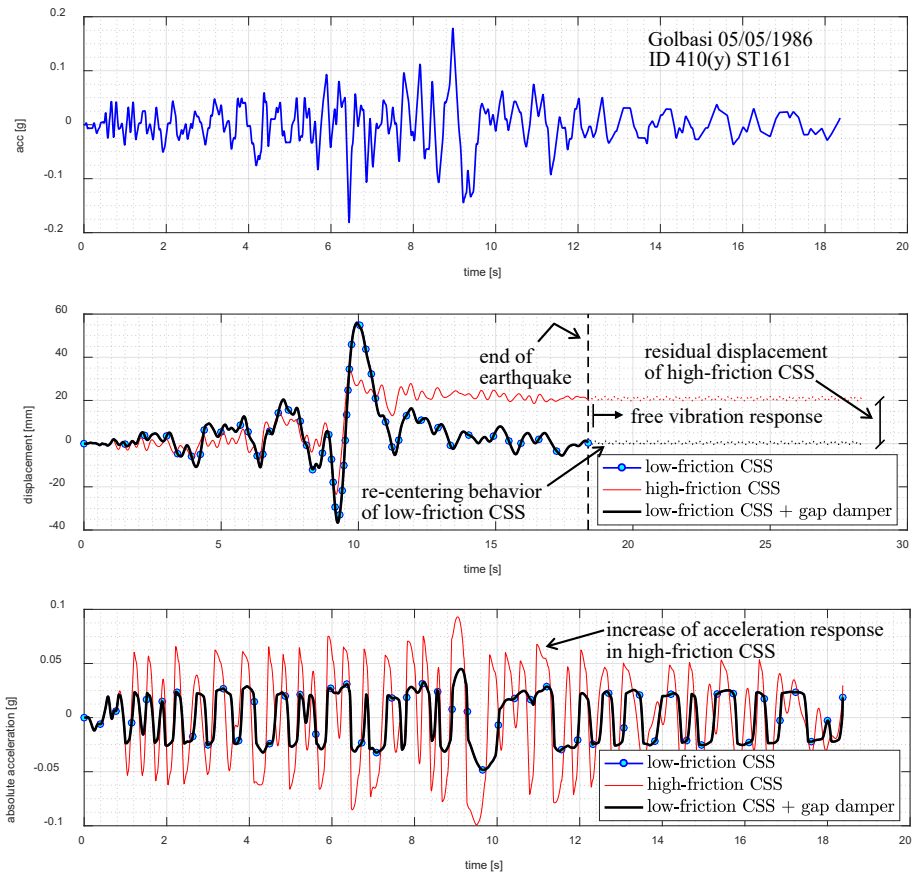

Fig. 7 – Low-intensity ground motion acceleration (top), displacement response for three different isolation layouts, including the proposed system (middle) and acceleration response (bottom) (adapted from [18])

5. Conclusions

A combined isolation system coupling low-friction FP bearings and a gap damper system has been presented in this paper. The proposed isolation system exploits the phased behavior of the gap damper, which offers supplemental damping only when the displacement of the isolators exceeds a pre-defined threshold called gap displacement, while it is not engaged for smaller values of the isolators' displacements. Such phased behavior is thus particularly convenient because it does not negatively affect the re-centering capabilities of the low-friction CSSs, while at the same time it offers an additional energy dissipation contribution that is necessary to mitigate the displacement demand during extreme earthquakes. The gap damper system has been designed according to a performance-oriented energy-based design procedure, assuming a simple elastic-perfectly plastic constitutive behavior under the assumption of a target displacement demand of the isolation system. Through a limited number of nonlinear response history analyses, it has been demonstrated that the proposed isolation system outperforms both low-friction and high-friction CSS isolation systems. Indeed, the gap dampers avoid undesirable effects such as high accelerations and high residual displacements obtained by high-friction CSS isolation systems during low-to-moderate intensity ground motions. At the same time, the gap dampers significantly mitigate the displacement demand of low-friction CSS isolation systems during extreme earthquakes, and the value of the target displacement demand can be designed by suitably selecting the yield force of the gap dampers according to the closed-form design expression proposed in this paper. The effect of the cumulative damage and of the gap displacement have also been investigated numerically. It has been found that the cumulative damage induced by the accumulated plastic deformation is detrimental for the performance of the gap damper system in terms of displacement reduction. In this context, it has been found that a proper design

choice is to assume the gap displacement equal to around 75% of the target reduced displacement, so as to minimize the cumulative damage effects. Otherwise, with smaller gap displacements the negative effects of the cumulative damage would be amplified during subsequent engagements. Moreover, the assumption of a larger gap displacement is also beneficial to avoid the increase of superstructure accelerations for low-to-moderate intensity earthquakes.

6. Acknowledgements

The authors acknowledge the support provided by the Italian Department of Civil Protection (DPC) in the framework of the national Research Project DPC – ReLUIS 2019/21, Work Package 15, Isolation and Dissipation.

6. References

[1] Zayas V, Low S, Mahin S (1987): The FPS earthquake resisting system. Report No. CB/EERC-87/01, Earthquake Engineering Research Center, University of California, Berkeley, 1987.

[2] Fenz DM, Constantinou MC (2006): Behaviour of the double concave Friction Pendulum bearing. *Earthquake Engineering & Structural Dynamics*, **35**(11), 1403–1424.

[3] Anagnostopoulos SA, Spiliopoulos KV (1992): An investigation of earthquake induced pounding between adjacent buildings. *Earthquake Engineering & Structural Dynamics*, **21**(4), 289-302.

[4] Panchal VR, Jangid RS (2009). Seismic response of structures with variable friction pendulum system. *Journal of Earthquake Engineering*, **13**(2), 193–216.

[5] Lu LY, Lee TY, Yeh SW (2009). Theory and experimental study for sliding isolators with variable curvature. *Earthquake Engineering and Structural Dynamics*, **40**(14), 1609–1627.

[6] Taniguchi T, Der Kiureghian A, Melkumyan M (2008): Effect of tuned mass damper on displacement demand of base-isolated structures. *Engineering Structures*, **30**, 3478-3488.

[7] De Domenico D, Ricciardi G (2018): Earthquake-resilient design of base isolated buildings with TMD at basement: Application to a case study. Soil Dynamics and Earthquake Engineering, **113**, 503-521.

[8] De Domenico D, Ricciardi G (2018): An enhanced base isolation system equipped with optimal Tuned Mass Damper Inerter (TMDI). *Earthquake Engineering & Structural Dynamics*, **47**, 1169-1192.

[9] De Domenico D, Ricciardi G (2018): Optimal design and seismic performance of tuned mass damper inerter (TMDI) for structures with nonlinear base isolation systems. *Earthquake Engineering & Structural Dynamics*, **47**(12), 2539-2560.

[10] Peng Y, Ding L, Chen J (2019): Performance evaluation of base-isolated structures with sliding hydromagnetic bearings. Structural Control and Health Monitoring, **26**(1), e2278.

[11] Peng Y, Huang T (2019): Sliding implant-magnetic bearing for adaptive seismic mitigation of base-isolated structures. Structural Control and Health Monitoring, **26**(10), e2431.

[12] Ponzo FC, Di Cesare A, Leccese G, Nigro D (2017): Shake table testing on restoring capability of double concave friction pendulum seismic isolation systems. *Earthquake Engineering & Structural Dynamics*, **46**(14), 2337-2353.

[13] Quaglini V, Gandelli E, Dubini P (2017): Experimental investigation of the re-centring capability of curved surface sliders. *Structural Control and Health Monitoring*, **24**(2), e1870.

[14] Quaglini V, Gandelli E, Dubini P, Limongelli MP (2017): Total displacement of curved surface sliders under nonseismic and seismic actions: A parametric study. *Structural Control and Health Monitoring*, **24**(12), e2031.

[15] Zargar H, Ryan KL, Marshall JD (2013): Feasibility study of a gap damper to control seismic isolator displacements in extreme earthquakes. *Structural Control and Health Monitoring*, **20**(8), 1159-1175.

[16] Rawlinson TA, Marshall JD, Ryan KL, Zargar H (2015): Development and experimental evaluation of a passive gap damper device to prevent pounding in base-isolated structures. *Earthquake Engineering & Structural Dynamics*, **44**(11), 1661-1675.

[17] Zargar H, Ryan KL, Rawlinson TA, Marshall JD (2017): Evaluation of a passive gap damper to control displacements in a shaking test of a seismically isolated three-story frame. *Earthquake Engineering & Structural Dynamics*, **46**(1), 51-71.

[18] De Domenico D, Gandelli E, Quaglini V (2020): Effective base isolation combining low-friction curved surface sliders and hysteretic gap dampers. *Soil Dynamics and Earthquake Engineering*, **130**, 105989.

[19] De Domenico D, Ricciardi G, Takewaki I (2019): Design strategies of viscous dampers for seismic protection of building structures: a review. *Soil Dynamics and Earthquake Engineering*, **118**, 144-165.

[20] McKenna F, Fenves GL, Scott MH, Jeremic B (2000): Open System for Earthquake Engineering Simulation (OpenSees), Pacific Earthquake Engineering Research Center (PEER), Berkeley, USA 2000.

[21] Constantinou M, Mokha A, Reinhorn AR (1990): Teflon bearings in base isolation II: modeling. *Journal of Structural Engineering*, **116**(2), 455–474.

[22] NTC2018. CSLLPP - Consiglio Superiore dei Lavori Pubblici. Norme Tecniche per le Costruzioni. Gazzetta Ufficiale 495 della Repubblica Italiana, No. 42 of 20 February 2018. Rome, Italy, (in Italian).

